ROTATIONAL OPTICAL ALIGNMENT FOR ARRAY BASED FREE SPACE BOARD-TO-BOARD OPTICAL INTERCONNECT WITH ZERO POWER HOLD

Jeffrey Chou[1], Kyoungsik Yu[1], Teymur Bakhishev[1], David Horsley[2], Robert Walmsley[3], Sagi Mathai[3], Mike Tan[3], S.Y. Wang[3], Vivek Subramanian[1], Ming Wu[1]
[1]University of California, Berkeley, USA
[2]University of California, Davis, USA
[3]Hewlett-Packard Laboratories, USA

ABSTRACT

We present an electrothermally actuated, rotating microlens array for the application of aligning free-space optical interconnects. A bistable mechanical brake holds the rotating stage after alignment so it does not consume any power in steady state. A 4×4 double-sided microlens array is fabricated via micro-inkjet printing and is precisely mounted on the lens shuttle with alignment bumps. Our MEMS device has a maximum rotation angle of 2.3° at an average velocity of 5.75°/s, and is capable of correcting angular misalignment of the laser/photodetector array chips. Measured CCD images of a 1×4 VCSEL array are presented to demonstrate the function of the device.

INTRODUCTION

Free-space optical interconnects with arrays of high-speed vertical cavity surface emitting lasers (VCSELs) and photodetectors can greatly enhance the bandwidth of current copper-based board-to-board interconnects [1]. However, small misalignments between the transmitting and receiving arrays will severely degrade the quality of optical communication channels. To overcome such issues, previous attempts provide dynamic solutions to correct for vibrations and other mechanical noises [2]. However, recent experimental results found dynamic misalignments in blade server systems to be negligible, while very low frequency static misalignment to be the primary source of communication loss [1].

To overcome this issue, our previous results demonstrated a 1-D electrothermal linear lens scanner and telecentric optical setup to correct for lateral shifts and board tilting, as shown in Fig. 1(a) [3]. This paper solves a third source of misalignment, which comes from rotational misalignments between arrays due to fabrication and assembly errors. Shown in Fig. 1(b), a 4×4 microlens array with a matched pitch VCSEL array is integrated on a MEMS rotary stage. The rotary stage is actuated by an electrothermal stepper motor, and can be locked by MEMS bistable brakes after alignment to minimize power consumption.

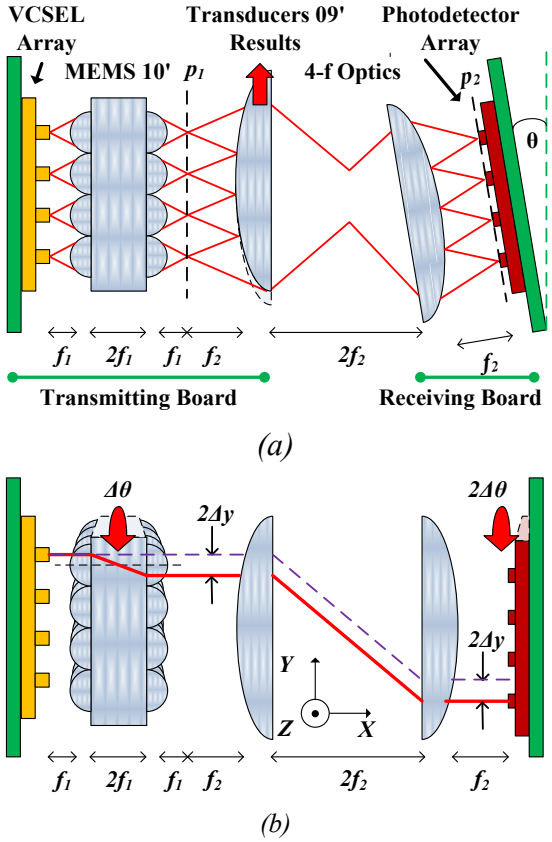

Fig. 1. a) Schematic view of the board-to-board optical setup with tilt and lateral displacement correction. b) Rotational correction about the X axis by Δθ, the final spot image is rotated by 2Δθ. Both schemes are designed to operate simultaneously, allowing up to 5 degrees of freedom of correction.

978-1-4244-5764-9/10/$26.00 ©2010 IEEE

OPTICAL SYSTEM

Figure 1b shows the VCSEL array is optically rotated about the X-axis on the plane p_1 by rotating a double-sided 4×4 microlens array, with diameter D_1=250 µm, focal length f_1=250 µm, and gap spacing $2f_1$=500 µm. A second 4-*f* optical system, with dimensions D_2= 6.325 mm and f_2=13.86 mm, is used to eliminate lateral misalignment and to relay the VCSEL array image to the plane p_2. Figure 1b illustrates that if the microlens array is shifted down by -Δy, a shift of -2Δy is generated at the plane p_2. As a result, for small angles, we get approximately a factor of 2 enhancement in rotation on the imaging plane p_2, thus doubling our angular displacement. The rotary stage can be cascaded with the previously reported translation stage [3] to correct for five degrees of freedom: tilt, rotations about the X axis, and translations in the X, Y and Z direction in board-to-board free-space parallel optical interconnects.

MEMS AND LENS DESIGN

A schematic of the MEMS device is shown in Fig. 2. Two pairs of U-shaped thermal actuators are located directly across the circular stage from each other, and are used to pivot the circular shuttle around the center by using a push and grip scheme [4]. Electrothermal actuators are chosen for their high force and low area advantages, which are needed to move large bulk optical components. By passing current through the U-shaped actuator, the thin beam heats up to about 1200°K, according to our simulations, thermally expands, and causes the entire structure to bend away from the thin beam. Based on our previously published results, the U-shaped actuators have a pushing force of 1.6 mN [3]. A rotationally compliant spring is designed for equal compliance in the wafer plane.

Once in position, the stage can be held in place without dissipating any power with bistable mechanical brakes, which are toggled digitally using similar U-shaped thermal actuators [3]. The brakes have a holding force of at least 1.6 mN. The same actuators are used for both rotation and brake toggling. A multiple input/out digital voltage data acquisition board is used to control all thermal actuators. Triangular teeth with a 3 µm pitch are patterned at the sidewalls of the brakes and stepper motors to increase the frictional forces.

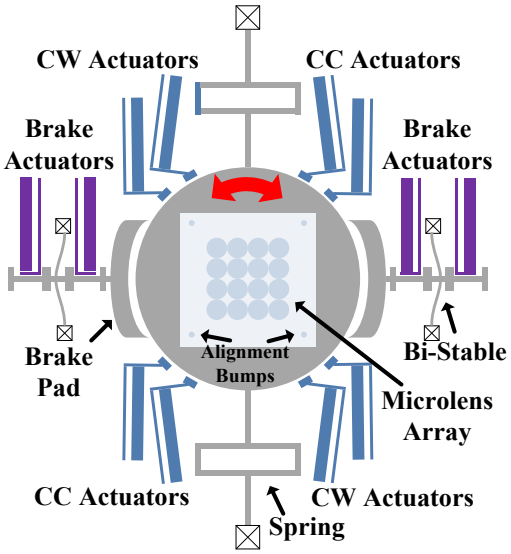

Fig. 2. Schematic of MEMS microlens array rotational stage. Clockwise (CW) and counter-clockwise (CC) actuators rotate the lens array.

FABRICATION

The MEMS rotational scanner is fabricated by bulk micromachining a 6-inch silicon-on-insulator (SOI) wafer with a 50µm device layer; the details of the device and fabrication are shown in Fig. 3. A single mask is used to define the entire MEMS structure via a front-side deep reactive ion etch (DRIE). A hydrofluoric acid vapor (HF vapor) release etch is used to remove the sacrificial oxide layer. Finally the double sided microlens array is assembled to the MEMS with an ultraviolet (UV) curable polymer.

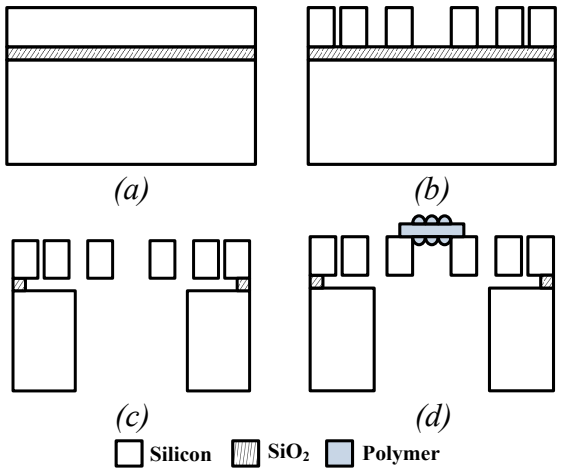

Fig. 3. Fabrication process flow of the MEMS device. a) SOI wafer with 50 µm device layer, and 2 µm buried oxide layer. b) DRIE entire front side device, single mask. c) HF vapor release etch. d) Mount fabricated microlens array onto the MEMS device with UV curable epoxy.

The double sided microlens array was fabricated via micro-inkjet printing of a low viscous UV curable polymer onto diced glass chips (1.9 mm × 1.9 mm) with spin-on Teflon patterns; details of the fabrication are shown in Fig. 4 [5]. A Teflon layer thickness of approximately 100 nm was spun onto the glass wafer. To prevent photoresist from slipping off of the Teflon, a 5 second O_2 plasma etch was used to roughen the surface and make it less hydrophobic. Etching of the Teflon was achieved by a 1 minute O_2 plasma etch, and was made hydrophobic again after a 2 hour curing bake. After patterning and etching of the Teflon, the microlenses were first printed and cured on the top-side. The chip was flipped over, and the second layer of lenses were deposited and cured on the bottom side. The completed MEMS rotational stage with an integrated microlens array is shown in Fig. 5. Fine, automatic alignment of the microlens array to the MEMS stage was achieved by micro-bumps in the corners of the microlens array chip which correspond to the corners of the MEMS shuttle.

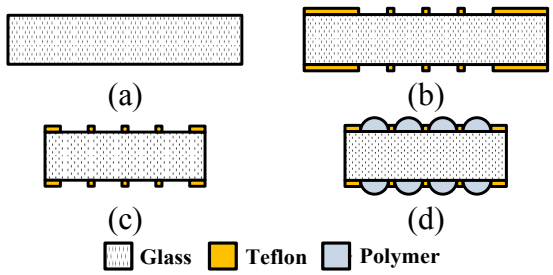

Fig. 4. Fabrication of a double-sided microlens array. a) Bare glass wafer. b) Coat and pattern front and backside with spin-on Teflon. c) Dice wafer. d) Deposit microlenses on front and back side.

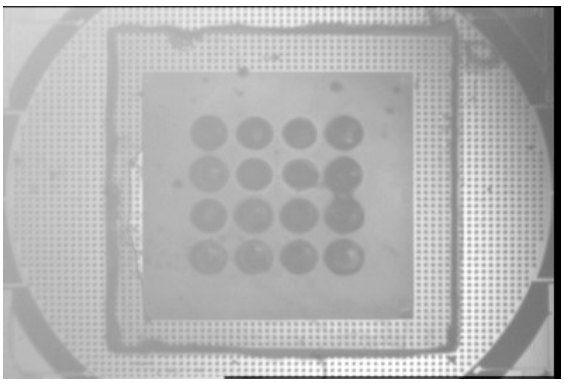

Fig. 5. Image of microlens array mounted on MEMS stage. Alignment is achieved with corner micro-bumps.

EXPERIMENTAL RESULTS

Images from video clips of the MEMS in motion are shown in Fig. 6. We see in Fig. 6(a), the MEMS shuttle is rotated by a maximum of 2.3°, and in Fig. 6(b) the bistable mechanical brake is engaged and holding the shuttle at a constant angle. Rotational displacement data taken from the video data as a function of time are shown in Fig. 7. The MEMS has a full rotation of 2.3° with an average velocity of 5.75°/s. This maximum displacement is currently limited by the spring design, and can theoretically achieve much larger angular displacement with more compliant springs. For a 10×10 high speed detector array with a pitch of 250μm and a detector area half width of 10 μm, a rotation above ±0.46° will cause signal loss. Thus, with a factor of 2 enhancement from the optics, we increase the acceptable rotational error by a factor of 5.

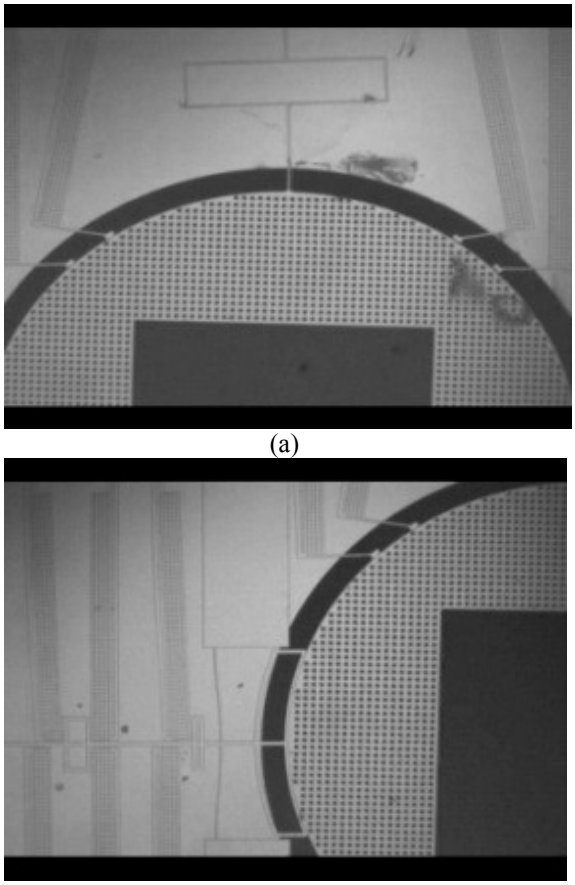

Fig.6. a) MEMS stage rotation at full 2.3° clockwise. b) Brake engaged to hold the stage at a constant rotational angle while dissipating zero power.

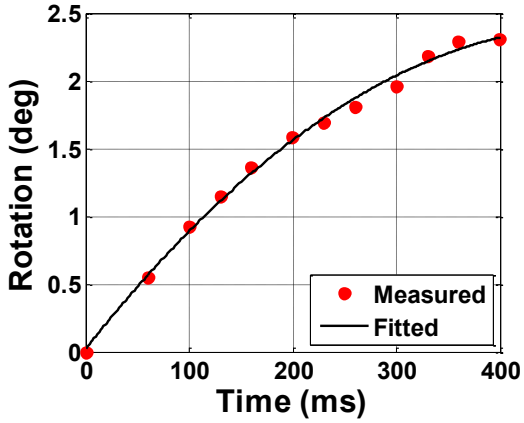

Fig. 7. MEMS rotation as a function of time. A maximum displacement of 2.3° is achieved. A quadratic best fit curve is fitted to the data.

To demonstrate the spot image rotation capabilities of the microlens array in Fig. 1, Fig. 8 shows a plot of the rotated image as a function of the rotation of the microlens array. Due to the imperfect fabrication of the microlens focal lengths, the factor of 2 rotational displacement enhancement is reduced to a factor of 4/3. Figure 9 shows a 1×4 VCSEL array image rotated by 4°, when the microlens array is rotated by 3°.

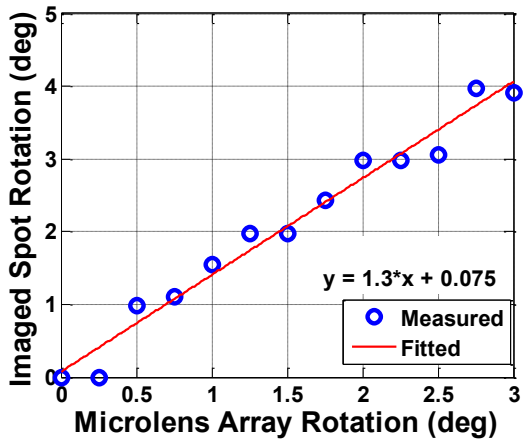

Fig. 8. Measured rotation of VCSEL array spots as a function of the microlens array rotation.

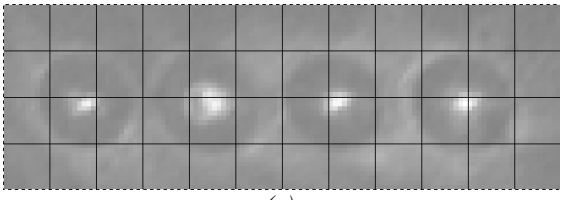

(a)

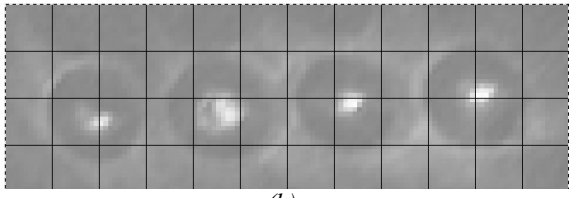

(b)

Fig. 9. Rotated spot images with double-sided microlens array. a) Image with a 0° rotation. b) Image with a 4° rotation at a microlens rotation of 3°.

CONCLUSION

We successfully demonstrate a rotating MEMS stage capable of supporting a millimeter-scale microlens array. A maximum mechanical rotation of 2.3° is achieved, with a theoretical imaged rotation of 4.6°. With a 10x10 arrayed detector radius of 10μm, we expand on the rotation alignment tolerance by a factor of 5. Custom double-sided microlenses were fabricated via inkjet printing, with a numerical aperture of about 0.5. Our full optical system for free-space interconnects is capable of simultaneous alignment along five degrees of freedom without consuming steady state power.

REFERENCES

[1] H. Kuo, P. Rosenberg, R. Walmsley, S. Mathai, L. Kiyama, J. Straznicky, M. Mclaren, M. Tan, and S. Wang, "Free-space optical links for board-to-board interconnects," *Applied Physics A: Materials Science & Processing*, vol. 95, Jun. 2009, pp. 955-965.

[2] J. Chou, K. Yu, D. Horsley, B. Yoxall, S. Mathai, M. Tan, S. Wang, and M. Wu, "Robust free space board-to-board optical interconnect with closed loop MEMS tracking," *Applied Physics A: Materials Science & Processing*, vol. 95, Jun. 2009, pp. 973-982.

[3] J. Chou, K. Yu, D. Horsley, S. Mathai, B. Yoxall, M. Tan, S. Wang, and M. Wu, "Electrothermally Actuated Free Space Board-to-Board Optical Interconnect with Zero Power Hold," *Proceedings of Transducers*, Denver Colorado: 2009, pp. 2202-2205.

[4] J.H. Comtois and V.M. Bright, "Applications for surface-micromachined polysilicon thermal actuators and arrays," *Sensors & Actuators: A. Physical*, vol. 58, 1997, pp. 19–25.

[5] H. Choo and R.S. Muller, "Optical properties of microlenses fabricated using hydrophobic effects and polymer-jet-printing technology," *2003 IEEE/LEOS International Conference on Optical MEMS and Their Applications*, 2003, pp. 169–170.